References

[1]Saksena, V.R., O'Reilly, J., and Kokotovic, P.V., "Singular Perturbations and Time-Scale Methods in Control Theory: Survey," *Automatica,* Vol. 220, 1984, pp. 273–293.

[2]Naidu, D.S. and Rao, A.K., "Singular Perturbation Analysis of Discrete Control Systems," *Lecture Notes in Mathematics,* Vol. 1154, Springer-Verlag, Berlin, 1985.

[3]Mahmoud, M.S. and Singh, M.G., *Large Scale Systems Modeling,* Pergamon Press, Oxford, 1981.

[4]Kando, H. and Iwazumi, T., "Initial Value Problems of Singularly Perturbed Discrete Systems Via Time-Scale Decomposition," *International Journal of Systems Science,* Vol. 14, 1983, pp. 555–570.

[5]Naidu, D.S. and Price, D.B., "Time Scale Synthesis of a Closed-loop Discrete Optimal Control System," *Journal of Guidance, Control, and Dynamics,* Vol. 10, Sept.-Oct. 1987, pp. 417–421.

Extensional Oscillations of Tethered Satellite Systems

A. K. Misra*
McGill University,
Montreal, Quebec, Canada
and
V. J. Modi†
University of British Columbia,
Vancouver, British Columbia, Canada

Introduction

RECENTLY, there has been considerable interest in the use of tethers in space. This has led to many investigations of their dynamics and control, but with a few exceptions, they usually deal with the rotational motion of the tether. However, during normal operations of tethered satellite systems, elastic oscillations of the tether, both transverse and longitudinal, are likely to be excited. The objective of this Note is to discuss some of the issues associated with longitudinal (extensional) oscillations of the tether. It may be pointed out that the resulting oscillations in tension may affect the attitude dynamics of the subsatellite significantly.

In their analysis of longitudinal oscillations of the tether, Banerjee and Kane[1] had assumed that the entire tether, including the undeployed part, undergoes extensional oscillations. In other words, friction between the tether and the reel, as well as that between different layers of the tether, was assumed to be negligible. This is termed the "total-slip" case in this Note. On the other hand, Misra and Modi,[2-3] Kohler et al.,[4] and Bergamaschi et al.[5] considered the other extreme case, in which it is assumed that there is sufficient friction so that the undeployed part of the tether does not undergo any extensional oscillation. This is referred to as the "no-slip" case here. The real case, of course, is somewhere in between. The present Note compares the results for the two extreme cases as well as those for intermediate levels of friction. It is shown that, even for very small friction, the results are quite close to those for the no-slip case. In addition, an analytical solution is presented for the no-slip case, while the previous investigators obtained the solutions numerically.

Presented as Paper 86-2274 at the AIAA/AAS Astrodynamics Conference, Williamsburg, VA, Aug. 18–20, 1986; received Oct. 14, 1986; revision received July 20, 1987.

*Associate Professor, Department of Mechanical Engineering.
†Professor, Department of Mechanical Engineering.

Formulation of the Problem

The system under consideration consists of the main orbiter A, subsatellite B, and the tether C (Fig. 1). It is assumed that the Shuttle is in a circular orbit having an orbital angular velocity Ω. A part of the tether is deployed, while the rest – the undeployed part – is wound around the tether reel. Only the longitudinal oscillations of the tether are considered. The reason for doing this is that the main objective of this work is to determine the role played by the undeployed part of the tether; however, the transverse vibrations are not affected by the undeployed part.

The longitudinal elastic deformation or stretch undergone by an element of the tether at any instant t is denoted by $v(s,t)$. Here, the coordinate s describes the position of the element measured along the "unstretched" tether from the point of its attachment to the reel, i.e., s is a material coordinate. The portion of the tether corresponding to $0<s<\ell_w$ is wrapped around the reel, while that corresponding to $\ell_w<s<\ell_t$ is the deployed part. Total deployed length is $\ell_d=\ell_t-\ell_w$.

Using the extended Hamilton's principle[6] (or otherwise), one can obtain the following equation of motion:

$$EA\frac{\partial^2 v}{\partial s^2}-\rho\frac{\partial^2 v}{\partial t^2}+3\rho\Omega^2[v+(s-\ell_w)]\,U(s-\ell_w)$$
$$+[1-U(s-\ell_w)]\,\{F+3\rho\Omega^2\,[(a/2)\sin(2s/a)]$$
$$+v\cos^2(s/a)]\}=0 \tag{1}$$

with the boundary conditions

$$v(0,t)=0 \tag{2a}$$

and

$$-EA\frac{\partial v}{\partial s}(\ell_t,t)-m_b\frac{\partial^2 v}{\partial t^2}(\ell_t,t)+3m_b\Omega^2[(\ell_t-\ell_w)$$
$$+v(\ell_t,t)]=0 \tag{2b}$$

Here, E and ρ stand for Young's modulus and mass per unit length of the tether, A the area of its cross section, a the radius of the tether reel, m_b the mass of the subsatellite, F the frictional force per unit length of the wrapped tether and a function of s, while $U(s-\ell_w)$ is the unit step function. In Eq. (1), the first two terms correspond to the classical string vibration problem, the third term is the gravity-gradient force corresponding to the deployed part of the tether, and the last term represents the friction and gravity-gradient force on the wrapped portion of the tether.

Equation (1) in conjunction with the boundary conditions (2) are now analyzed for the three cases of no slip, total slip, and intermediate slip, as described earlier.

Analysis and Results

Analysis for the No-Slip Case

In this case, the undeployed part is prevented from oscillating due to the presence of sufficient friction. Thus, $v(s,t)=0$ for $0<s<\ell_w$ and we need to consider only the

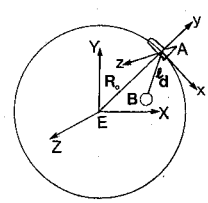

Fig. 1 Tethered Satellite System.

deployed part of the tether [i.e., $s > \ell_w$; $U(s-\ell_w)=1$]. It is convenient to nondimensionalize the equation of motion and the boundary conditions by defining

$$\eta = (s-\ell_w)/\ell_d, \quad \tau = \Omega t, \quad \psi(\eta,\tau) = v(s,t)/\ell_d$$

$$p^2 = EA/\rho\Omega^2\ell_d^2, \quad r = \rho\ell_d/m_b, \quad \ell_d = \ell_t - \ell_w \tag{3}$$

Here r is the mass ratio (deployed tether mass to subsatellite mass), while p is a measure of the ratios of frequencies of longitudinal oscillation to the orbital frequency. The equation of motion now becomes

$$p^2\frac{\partial^2\psi}{\partial\eta^2} - \frac{\partial^2\psi}{\partial\tau^2} + 3(\psi+\eta) = 0 \tag{4}$$

with the boundary conditions

$$\psi(0,\tau) = 0 \tag{5a}$$

and

$$-p^2 r\frac{\partial\psi}{\partial\eta}(1,\tau) - \frac{\partial^2\psi}{\partial\tau^2}(1,\tau) + 3[1+\psi(1,\tau)] = 0 \tag{5b}$$

In order to solve the set of Eqs. (4) and (5), one must put

$$\psi(\eta,\tau) = \psi_0(\eta) + \bar{\psi}(\eta,\tau) \tag{6}$$

Physically, ψ_0 represents the steady-state longitudinal extension of the tether, while $\bar{\psi}$ is the oscillation around this steady-state solution. Substitution of Eq. (6) into Eqs. (4) and (5) yields an ordinary differential equation for ψ_0 and a partial differential equation for $\bar{\psi}$ as follows:

$$p^2\frac{d^2\psi_0}{d\eta^2} + 3\psi_0 = -3\eta \tag{7}$$

with boundary conditions

$$\psi_0(0) = 0 \tag{8a}$$

and

$$-p^2 r\frac{d\psi_0}{d\eta}(1) + 3[1+\psi_0(1)] = 0 \tag{8b}$$

$$p^2\frac{\partial^2\bar{\psi}}{\partial\eta^2} - \frac{\partial^2\bar{\psi}}{\partial\tau^2} + 3\bar{\psi} = 0 \tag{9}$$

with boundary conditions

$$\bar{\psi}(0,\tau) = 0 \tag{10a}$$

and

$$-p^2 r\frac{\partial\bar{\psi}}{\partial\eta}(1,\tau) - \frac{\partial^2\bar{\psi}}{\partial\tau^2}(1,\tau) + 3\bar{\psi}(1,\tau) = 0 \tag{10b}$$

The solution to Eqs. (7) and (8) is given by

$$\psi_0 = C\sin[(\sqrt{3}/p)\eta] - \eta \tag{11}$$

where

$$C = (rp/\sqrt{3})/[r\cos(\sqrt{3}/p) - (\sqrt{3}/p)\sin(\sqrt{3}/p)] \tag{12}$$

Note that the equilibrium tension at any point η is given by

$$T_0 = EA\frac{d\psi_0}{d\eta} = EA\{C(\sqrt{3}/p)\cos[(\sqrt{3}/p)\eta] - 1\} \tag{13}$$

Thus, in general, the equilibrium stretch and tension vary sinusoidally along the tether. However, for all the tethered satellites planned for the near future, p is much larger than 1. (For TSS-1, p is approximately 80.) Hence, ψ_0 and T_0 are described by only small parts of sinusoidal waves, which may be approximated by polynomials. It can be shown that, if $p \gg 1$, the limiting values of v_0 ($= \ell_d\psi_0$) and T_0 are given by

$$v_0 = (3m_b\Omega^2\ell_d^2/EA)[\eta + (r/2)(\eta - \eta^3/3)] \tag{14}$$

and

$$T_0 = 3m_b\Omega^2\ell_d^2[1 + (r/2)(1-\eta^2)] \tag{15}$$

The homogeneous partial differential equation (9) with boundary conditions (10) can be solved to yield the frequency equation

$$\tan[(3+\lambda^2)^{1/2}/p] = rp/(3+\lambda^2)^{1/2} \tag{16}$$

where λ_n represents the nth longitudinal frequency divided by Ω. The corresponding eigenfunctions are given by

$$\phi_n(\eta) = \sin[\eta(3+\lambda^2)^{1/2}/p] \tag{17}$$

It may be interesting to compare the frequency equation and the eigenfunction above to that of the tether-subsatellite system on the surface of the Earth. For the latter case, the frequency equation is $\beta\tan\beta = r$ and the eigenfunction is $\sin(\beta_n\eta)$, where $\beta = \lambda/p$. The presence of the gravity gradient leads to an addition of 3 to λ^2, which results in a slight reduction of frequencies in the orbiting case.

Results for the No-Slip Case

In order to obtain some quantitative results, a tether having the same parameters as that in Ref. 1 is considered: the area of cross section is $\pi \times 10^{-6}$ m^2, elastic modulus is 4.488×10^{10} N/m^2, and mass per unit length is 4.09×10^{-3} kg/m. The orbital altitude is assumed to be 400 km and the subsatellite mass is 450 kg.

The variation of the two lowest longitudinal frequencies with the deployed length is given in Fig. 2. It may be noted

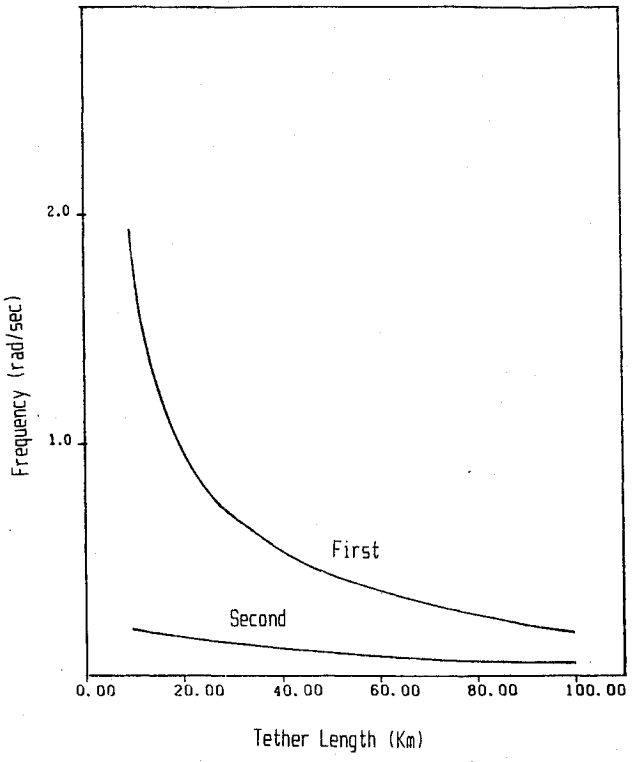

Fig. 2 Variation of the two lowest longitudinal frequencies with the deployed length.

that the lowest natural frequency does not vary as much with the deployed length as the second one. In fact, it can be shown that the lowest frequency varies approximately as $\ell_d^{-1/2}$ while the higher ones are proportional to ℓ_d^{-1}. It can also be seen from Table 1 that only the lowest natural frequency is affected by the subsatellite mass while the others are almost independent of it.

If the tether is modeled as a massless spring, the corresponding frequency of oscillation of the tether-subsatellite system is given by $[EA/m_b\ell_d]^{1/2}$. When this frequency is compared with the more accurate frequency (lowest) obtained from the solution of Eq. (16), one notes that the difference is small for satellites having larger mass but can be significant for smaller subsatellites (Table 2).

Total-Slip Case

If the friction between the tether and the reel and between the adjacent layers of the tether is negligible, the entire tether undergoes extensional oscillations. This is clearly unrealistic. However, for the sake of completeness, total slip is considered later as a special case of partial slip.

Analysis for the Partial-Slip Case

This is the most realistic situation. In order to develop a solution for this case, the effect of friction must be examined. If the tension in any element of the tether wrapped on the reel is sufficient to overcome the static friction F_s, then that element undergoes longitudinal extension; otherwise, the element remains static. The static friction, of course, depends on the tether and drum materials and the number of turns of the tether on the drum. The friction is assumed to be of coulomb type.

The variation of tension along the wrapped portion of the tether is modeled here in a manner similar to a common capstan-rope situation. Thus, the tension along the wrapped tether varies with the wrapping angle as

$$T = T_r \exp(-\mu\delta) \tag{18}$$

where μ is the friction coefficient and T_r the tension in the tether as it leaves the reel. If on an element of the tether $T > F_s$, the element undergoes extensional oscillation. Using this criterion, one can determine the "partial" oscillating length ℓ_p as follows:

$$\ell_p = \ell_d + (a/\mu)\,\ell n(T_r/F_s) \quad \text{if } \mu \neq 0 \tag{19a}$$

$$= \ell_t, \text{ if } \mu = 0 \tag{19b}$$

If μ is very large, $\ell_p \approx \ell_d$.

It is more convenient to redefine the nondimensional variables as follows:

$$\tau = \Omega t, \quad \eta = s'/\ell_p, \quad \psi(\eta,\tau) = v(s',t)/\ell_p$$

$$s' = s - (\ell_t - \ell_p), \quad p^2 = EA/\rho\Omega^2\ell_p^2, \quad r = \rho\ell_p/m_b \tag{20}$$

Furthermore, to carry out a Rayleigh-Ritz discretization, one can expand $\psi(\eta,\tau)$ in series form as

$$\psi(\eta,\tau) = \sum_{i=1}^{N} \eta^i C_i(\tau) \tag{21}$$

Substituting in the variational form of the Hamilton's principle, one can obtain, after some algebra, the discretized equations governing the longitudinal oscillations as follows:

$$[M]\{\ddot{C}\} + [K]\{C\} = \{Q\} \tag{22}$$

Here the elements of the matrices $[M]$, $[K]$, and $\{Q\}$ are given by

$$m_{ij} = 1 + r/(i+j+1) \tag{23a}$$

$$k_{ij} = p^2 r[ij/(i+j-1)]$$

$$-3[1 + r(1-\alpha^{i+j+1})/(i+j+1) - rg_{ij}] \tag{23b}$$

$$Q_i = 3(1-\alpha) + 3r[(1-\alpha^{i+2})/(i+2)$$

$$-\alpha(1-\alpha^{i+1})/(i+1)] - (3r/2\beta)\,\gamma_i + F_i \tag{23c}$$

where

$$g_{ij} = \int_0^{\alpha} \eta^{i+j} \cos^2[\beta(\eta - 1 + \ell_t/\ell_p)]\,d\eta \tag{23d}$$

Table 1 Variation of frequencies of longitudinal oscillations (in radians/second) with the subsatellite mass, for the no-slip case; deployed length = 60 km, orbital altitude = 400 km

	Satellite mass, kg				
Mode	100	300	500	700	900
1	0.1112	0.0781	0.0634	0.0547	0.0488
2	0.3644	0.3307	0.3219	0.3179	0.3157
3	0.6495	0.6273	0.6224	0.6203	0.6191
4	0.9466	0.9307	0.9273	0.9259	0.9251

Table 2 Comparison of the lowest natural frequency obtained from Eq. (16) with that of an idealized spring-mass system

Satellite mass	100	300	500	700	900
Frequency of a spring-mass system (rad/s)	0.1533	0.0885	0.0686	0.0579	0.0511
Solution of Eq. (16) (rad/s) II	0.1112	0.0781	0.0634	0.0547	0.0488
Percentage difference 100 × (I − II)/II	37.9	13.3	8.2	5.9	4.7

Table 3 Frequencies (in radians/second) for various friction coefficients; deployed length = 1 km, wrapped length = 99 km, subsatellite mass = 450 kg

μ	0 (total slip)	0.0001	0.001	0.01	0.1	Large (no slip)
ℓ_p, km	100	35.50	4.45	1.345	1.0345	1.0
Frequencies:						
1	0.0487	0.0892	0.2636	0.4817	0.5495	0.5588
2	0.1998	0.5360	4.1619	13.7311	17.8473	18.4561
3	0.3773	1.0479	8.3010	27.4447	35.6796	36.8975
4	0.5602	1.5676	12.4652	41.2284	53.6011	55.4311
5	0.8390	2.3496	18.6903	61.8198	80.3723	83.1162

$$\gamma_i = \int_0^{\alpha} \eta^i \sin[2\beta(\eta - 1 + \ell_t/\ell_p)]\eta \qquad (23e)$$

$$F_i = \int_0^{\alpha} \eta^i F(\eta) d\eta \qquad (23f)$$

$$\alpha = (\ell_p - \ell_d)/\ell_p, \quad \beta = \ell_p/a \qquad (23g)$$

The frequencies of longitudinal oscillations can now be determined by solving the eigenvalue problem obtained from Eq. (22).

Results for the Partial-Slip Case

The friction affects the natural frequencies by governing the oscillating length ℓ_p. [Note that, in Eq. (23b), $p^2 r = EA/m_b\Omega^2\ell_p$ and $r = \rho\ell_p/m_b$]. The second row of Table 3 shows the oscillating length ℓ_p for a given friction coefficient μ. The table corresponds to a deployed length of 1 km and a wrapped length of 99 km. The orbital altitude is 220 km and the subsatellite mass is 450 kg. The tether parameters are as given in the no-slip case, while the diameter of the reel (i.e., $2a$) is 1 m. It is assumed that F_s is 0.1% of T_r.

It may be noted in Table 3 that, as the friction increases, the oscillating length ℓ_p reduces and the frequencies increase. Between the two extreme cases, the first natural frequency changes by an order of magnitude, while the others change by two orders of magnitude for the particular case considered. It may also be noted that, even when μ is only moderately high (0.1), the frequencies are quite close to the no-slip case.

It may also be observed from Table 3 that the lowest natural frequency can be an order of magnitude smaller compared to the rest, while the second, third, ..., natural frequencies are roughly proportional to 1,2,..., etc., respectively. As has been mentioned earlier, in the first mode, the tether behaves approximately as a spring having a mass attached to its end; in the other modes, the tether behaves as a bar vibrating axially with the end mass playing a relatively minor role.

Concluding Remarks

Longitudinal oscillation of tethered satellite systems for various levels of friction acting on the undeployed portion of the tether was studied. It was noted that, for large undeployed lengths, there can be significant differences in the frequencies for various levels of friction; however, if the friction is moderately high, the longitudinal frequencies approach those of the no-slip case, and one can use the analytical solution for that case presented in this Note in most situations.

Acknowledgment

The investigation reported here was supported by the Natural Sciences and Engineering Research Council of Canada under Grants A-0967 and A-2181.

References

[1]Banerjee, A.K. and Kane, T.R., "Tether Deployment Dynamics," *The Journal of the Astronautical Sciences*, Vol. 30, Oct.-Dec. 1982, pp. 347-365.

[2]Misra, A.K. and Modi, V.J., "A General Dynamical Model for the Space Shuttle Based Tethered Subsatellite System," *Advances in the Astronautical Sciences*, Vol. 40, Pt. II, 1979, pp. 537-557.

[3]Misra, A.K., Xu, D.M., and Modi, V.J., "On Vibrations of Orbiting Tethers," *Acta Astronautica*, Vol. 13, Oct. 1986, pp. 587-597.

[4]Kohler, P. et al., "Dynamics of a System of Two Satellites Connected by a Deployable and Extensible Tether of Finite Mass," Contract Rept. ESTEC Contract 2992/76/NL/AK(SC), Vols. 1 and 2, Oct. 1978, pp. 15-22.

[5]Bergamaschi, S., Cusinato, S., and Sinopoli, A., "A Continuous Model for Tether Elastic Vibrations in TSS," AIAA Paper 86-0087, Jan. 1986.

[6]Meirovitch, L., *Methods in Analytical Dynamics*, McGraw-Hill, New York, 1970, pp. 66-69.

Dynamic Simulation of Spin-Stabilized Spacecraft with Sloshing Fluid Stores

Daniel E. Hill* and Joseph R. Baumgarten†
Iowa State University, Ames, Iowa
and
John T. Miller†
Arnold Engineering Development Center, Tullahoma, Tennessee

Introduction

LAUNCHINGS of several communications satellites have consistently resulted in a nutating motion of the spacecraft. Flight data from the roll, pitch, and yaw axis rate gyros indicated a constant-frequency, equal-amplitude, sinusoidal oscillation about the pitch and yaw axis. The vector combination of these two components of oscillation resulted in a coning motion of the satellite about the roll axis. The vehicle was spin-stabilized at launch about the minor axis, having a one revolution per second (rps) roll angular velocity imparted to it.

After launching from the carrier vehicle in the perigee phase of its orbit, the satellite's perigee assist module (PAM) fired its thruster to establish a geosynchronous Earth orbit. It is this axial thrust that gives rise to the coning that predominates after PAM motor burnout. Consistently, flight data from rate gyros indicated the steady-state one-half cycle per second (cps) coning frequency and a one-half cycle cps small-amplitude disturbance superimposed on the 1 rps roll angular velocity.

Combustion instabilities in the PAM rocket motor were suspected to be the source of a side force that would induce the coning motion. In order to investigate the presence of any such combustion instabilities, a PAM rocket motor was fired at the Engine Test Facility, Arnold Engineering Development Center, Arnold Air Force Station. A test fixture having lateral and axial load cells was utilized, allowing the PAM to be spun at 1 rps during firing. A spectral analysis was completed of the resulting load cell records obtained during firing. The test results indicated no forces at the required frequency (one-half cps), and it was concluded that combustion instabilities were not the source of moments causing coning motion.

A preliminary analysis of the payload (communication satellite) was completed indicating that sloshing fluid stores may induce the coning motion. It was suspected that sloshing motion of the liquid stores in the vehicle, excited by the axial thrust, was the mechanism for creating the nutation of the spacecraft.

The modeling of fluid slosh is extensive and has been used by researchers to study its effect on space vehicle motion.[1-3] Michelini et al.[4] outlined a procedure for developing the equations of motion of a spinning satellite containing fluid stores. The equations of motion were not presented, but the study supplied the analytical background for the experimental identification of the dynamic model. Experimental results showed that small-amplitude free surface wave motion does not cause instabilities in the vehicle. Instabilities were found to be generated by the fundamental mode of fluid slosh, which is not excited by small-amplitude free surface wave motion. The consequence of the first-mode natural frequency causing instability in the vehicle justifies the use of an equivalent spherical pendulum model of fluid slosh.

Received May 15, 1986; revision received Nov. 3, 1987.

*Graduate Student; currently, Senior Engineer, Martin Marietta.
†Professor of Mechanical Engineering.
‡Research Engineer.